

lncRNA ITGB8-AS1 functions as a ceRNA to promote colorectal cancer growth and migration through integrin-mediated focal adhesion signaling

Xiaoting Lin,^{1,2,6} Shiwen Zhuang,^{1,2,6} Xue Chen,³ Jun Du,³ Longhua Zhong,¹ Jiancheng Ding,³ Lei Wang,³ Jia Yi,³ Guosheng Hu,³ Guohui Tang,⁴ Xi Luo,⁵ Wen Liu,³ and Feng Ye^{1,2}

¹Department of Medical Oncology, Xiamen Key Laboratory of Antitumor Drug Transformation Research, the First Affiliated Hospital of Xiamen University, Xiamen 361003, China; ²Department of Clinical Medicine, Fujian Medical University, Fuzhou 350122, China; ³Fujian Provincial Key Laboratory of Innovative Drug Target Research, School of Pharmaceutical Sciences, Xiamen University, Xiamen 361104, China; ⁴Department of Anus and Bowels, Affiliated Nanhua Hospital, University of South China, Hengyang 421010, China; ⁵BE/Phase I Clinical Center, First Affiliated Hospital of Xiamen University, Xiamen 361003 China

Long non-coding RNAs (lncRNAs) play critical roles in tumorigenesis and progression of colorectal cancer (CRC). However, functions of most lncRNAs in CRC and their molecular mechanisms remain uncharacterized. Here we found that lncRNA ITGB8-AS1 was highly expressed in CRC. Knockdown of ITGB8-AS1 suppressed cell proliferation, colony formation, and tumor growth in CRC, suggesting oncogenic roles of ITGB8-AS1. Transcriptomic analysis followed by KEGG analysis revealed that focal adhesion signaling was the most significantly enriched pathway for genes positively regulated by ITGB8-AS1. Consistently, knockdown of ITGB8-AS1 attenuated the phosphorylation of SRC, ERK, and p38 MAPK. Mechanistically, ITGB8-AS1 could sponge miR-33b-5p and let-7c-5p/let-7d-5p to regulate the expression of integrin family genes ITGA3 and ITGB3, respectively, in the cytosol of cells. Targeting ITGB8-AS1 using antisense oligonucleotide (ASO) markedly reduced cell proliferation and tumor growth in CRC, indicating the therapeutic potential of ITGB8-AS1 in CRC. Furthermore, ITGB8-AS1 was easily detected in plasma of CRC patients, which was positively correlated with differentiation and TNM stage, as well as plasma levels of ITGA3 and ITGB3. In conclusion, ITGB8-AS1 functions as a competing endogenous RNA (ceRNA) to regulate cell proliferation and tumor growth of CRC via regulating focal adhesion signaling. Targeting ITGB8-AS1 is effective in suppressing CRC cell growth and tumor growth. Elevated plasma levels of ITGB8-AS1 were detected in advanced-stage CRC. Thus, ITGB8-AS1 could serve as a potential therapeutic target and circulating biomarker in CRC.

INTRODUCTION

Colorectal cancer (CRC) is one of the most common gastrointestinal cancers and the leading cause of cancer-related death. Despite decreasing incidence of CRC in older populations, the incidence has nearly doubled in younger adults since the early 1990s.¹ Implementation of CRC screening programs has increased early detection

rates, but many CRC patients are still diagnosed at an advanced stage and often lose chances for curative resection.² In spite of great improvement achieved, currently available treatment choices and survival gains for advanced CRC remain limited. Thus, investigations of novel biomarkers and targets are urgently needed to improve outcomes of CRC.

Long noncoding RNAs (lncRNAs) represent a class of non-coding transcripts that are more than 200 nucleotides in length. Growing evidence has revealed lncRNA dysregulation across various cancer types, including CRC, and their indispensable roles in all cancer hallmarks.^{3–20} However, functions and mechanisms of most lncRNAs in CRC remain uncharacterized.³ Identifying CRC-related lncRNAs with transcriptomics for further functional validation is imperative.

Focal adhesion, localized on the basal surface of the epithelium, is a type of anchoring junction dominantly mediated by integrins that integrate surrounding extracellular matrix (ECM) with actin cytoskeleton. Focal adhesion starts with integrin allosteric conformational changes.^{21,22} Intriguingly, integrins are unique bidirectional signaling molecules. For inside-out signaling, Talin binds to the small cytoplasmic tails of integrins and triggers integrin conformational changes, followed by adaptor recruitment and downstream cascade activation.^{23,24} For outside-in signaling, integrin extracellular domain interacts with ECM ligands, followed by integrin clustering and

Received 24 November 2020; accepted 20 July 2021;

<https://doi.org/10.1016/j.ymthe.2021.08.011>.

⁶These authors contributed equally

Correspondence: Feng Ye, Department of Clinical Medicine, Fujian Medical University, Fuzhou 350122, China.

E-mail: yefengdoctor@xmu.edu.cn

Correspondence: Wen Liu, Fujian Provincial Key Laboratory of Innovative Drug Target Research, School of Pharmaceutical Sciences, Xiamen University, Xiamen 361104, China.

E-mail: w2liu@xmu.edu.cn

Correspondence: Xi Luo, BE/Phase I Clinical Center, First Affiliated Hospital of Xiamen University, Xiamen 361003 China.

E-mail: luoxi2999@163.com

protein hub accumulation to initiate downstream pathways, typically involving a series of phosphorylation events including FAK, SRC, and subsequent ERK and p38 MAPK phosphorylation.²⁴

Focal adhesion affects nearly all aspects of cell life.²⁵ Integrin signaling, likewise, regulates diverse functions in tumor cells, including proliferation, survival, migration, invasion, and stemness.^{26,27} As core components of focal adhesion, the integrin family comprises 24 transmembrane $\alpha\beta$ heterodimers generated from selective non-covalent associations between 18 α and 8 β subunits,²⁴ among which integrin $\beta 3$ plays a dominant role, and is associated with malignant phenotypes of tumors. Integrins can be classified into receptors recognizing Arg-Gly-Asp (RGD) peptide motifs, collagen receptors, laminin receptors, and leukocyte-specific integrins.^{24,27} While some integrins bind to only specific ECM ligands, others exhibit a broader ligand-binding repertoire.^{24,27} Distinct signaling in cancer can be triggered by different integrin heterodimers, and thus cancer cell behavior is determined by the pattern of integrin expression.^{24,27} Once integrins were activated, downstream cascades, including PI3K/AKT and MAPK pathways, were initiated to promote tumor survival and progression. Present on both tumor cells and tumor-associated host cells, integrins have a profound influence on tumor cells themselves and the tumor microenvironment.²⁶ lncRNA HOXD-AS1 suppresses CRC growth and metastasis through inhibiting HOXD3-induced integrin $\beta 3$ transcription.¹⁴ Nevertheless, whether and how lncRNAs regulate integrins, especially integrin-mediated focal adhesions, to regulate CRC remains largely unclear.

In the present study, we uncovered that ITGB8-AS1 sponged various microRNAs (miRNAs) to activate integrin $\alpha 3$ and $\beta 3$ transcription and focal adhesion signaling, which was required for CRC growth and migration. We also demonstrated that ITGB8-AS1 is highly expressed in CRC tissues and plasma, which could serve as a potential therapeutic target and predictive biomarker for CRC.

RESULTS

ITGB8-AS1 is required for CRC growth and migration

To screen potential oncogenic lncRNAs in CRC, our previous work compared lncRNA expression profiles in matched CRC and adjacent normal tissues using transcriptomic analysis. ITGB8-AS1, an uncharacterized lncRNA, was highly expressed in CRC tissues.²⁸ The expression of ITGB8-AS1 was examined in various CRC as well as normal colon epithelial cell lines, which revealed that, compared to the normal colon epithelial cell line ccc-HIE-2, most of the CRC cells presented a higher expression of ITGB8-AS1 (Figure S1). HCT116 and DLD-1 cells were chosen for further experiments. To investigate its biological functions in CRC, we knocked down ITGB8-AS1 with short hairpin RNAs (shRNAs) followed by CCK-8 assay, unveiling that knockdown of ITGB8-AS1 reduced cell proliferation (Figures 1A and 1B). Similar to CCK-8 results, a decrease in colony formation was observed in ITGB8-AS1-knockdown CRC cells (Figure 1C). To further determine *in vivo* effects of ITGB8-AS1 on CRC growth, equal numbers of ITGB8-AS1 stably knocked down HCT116 cells and their controls were subcutaneously injected into BALB/c nude mice, and tumor

weights were analyzed after sacrifice. Consistent with the *in vitro* findings, knockdown of ITGB8-AS1 inhibited CRC tumor growth (Figures 1D and 1E; Figure S2). Next, impacts of ITGB8-AS1 on migration capability of CRC cells were assessed. Transwell assays and wound-healing experiments revealed that knockdown of ITGB8-AS1 mitigated cell migration capability in CRC (Figures 1F and 1G). To further confirm roles of ITGB8-AS1 in CRC, overexpression of ITGB8-AS1 was then performed. As expected, ITGB8-AS1 overexpression promoted cell proliferation, colony formation, and migration in CRC, indicated by CCK-8, colony formation, Transwell, and wound-healing assays (Figure 2). Taken together, ITGB8-AS1 is highly expressed in CRC cells and played an oncogenic role in CRC.

Focal adhesion signaling is positively regulated by ITGB8-AS1 in CRC

To identify target genes and their relevant signaling pathways regulated by ITGB8-AS1, RNA sequencing (RNA-seq) was performed and gene expression profiles of siITGB8-AS1 and siCTL were compared. The impact of ITGB8-AS1 on gene expressions between two biological repeats was highly correlated (Figure S3). Specifically, there were 638 and 449 genes positively and negatively regulated by ITGB8-AS1, respectively (fold change > 1.5, $q < 0.05$) (Figures 3A and 3B; Table S1). The expression patterns of these ITGB8-AS1-regulated genes were shown by heatmap (Figure 3C). To gain insights into the biological functions and signaling pathways ITGB8-AS1 is involved in, KEGG pathway enrichment analysis was performed. Focal adhesion signaling was unveiled to be the most significantly enriched pathway for genes positively regulated by ITGB8-AS1 (Figure 3D). Western blots showed that knockdown of ITGB8-AS1 lowered phosphorylation levels of SRC, ERK, and p38 MAPK in CRC cells, supporting the regulation of focal adhesion signaling cascade by ITGB8-AS1 (Figure 3E).

ITGB8-AS1 functions as a miRNA sponge for miR-33b-5p and let-7d-5p/let-7d-5p to regulate the expression of integrins

To investigate the molecular mechanisms underlying ITGB8-AS1-regulated focal adhesion signaling, we first sought to clarify coding potential of ITGB8-AS1. Unlike ACTB, polysome profiling analysis showed that ITGB8-AS1 was enriched in free-RNA fractions, indicating that it has no coding capability (Figure 4A), which was further supported by CPAT and CPC, two web tools for predicting coding potential (Figure S4). The action mode of a lncRNA is largely associated with its subcellular localization. We therefore determined subcellular localization of ITGB8-AS1 using cellular fractionation assay followed by quantitative real-time PCR analysis. As manifested in Figure 4B, ACTIN and MALAT1 were mainly localized in the cytosol and nucleus of CRC cells, respectively, indicating effective cellular fractionation. Consistent with results of cellular fractionation assays, ITGB8-AS1 was predominantly localized in cytoplasm as presented by RNA-fluorescence *in situ* hybridization (FISH) (Figure 4C). ITGB8-AS1 was mainly localized in the cytosol, but a small portion was in the nucleus of CRC cells. Given that miRNA sponge is the most common route for cytoplasmic lncRNA to elicit biological functions, we constructed a competing endogenous RNA (ceRNA) network to bridge ITGB8-AS1 with focal-adhesion-related genes via

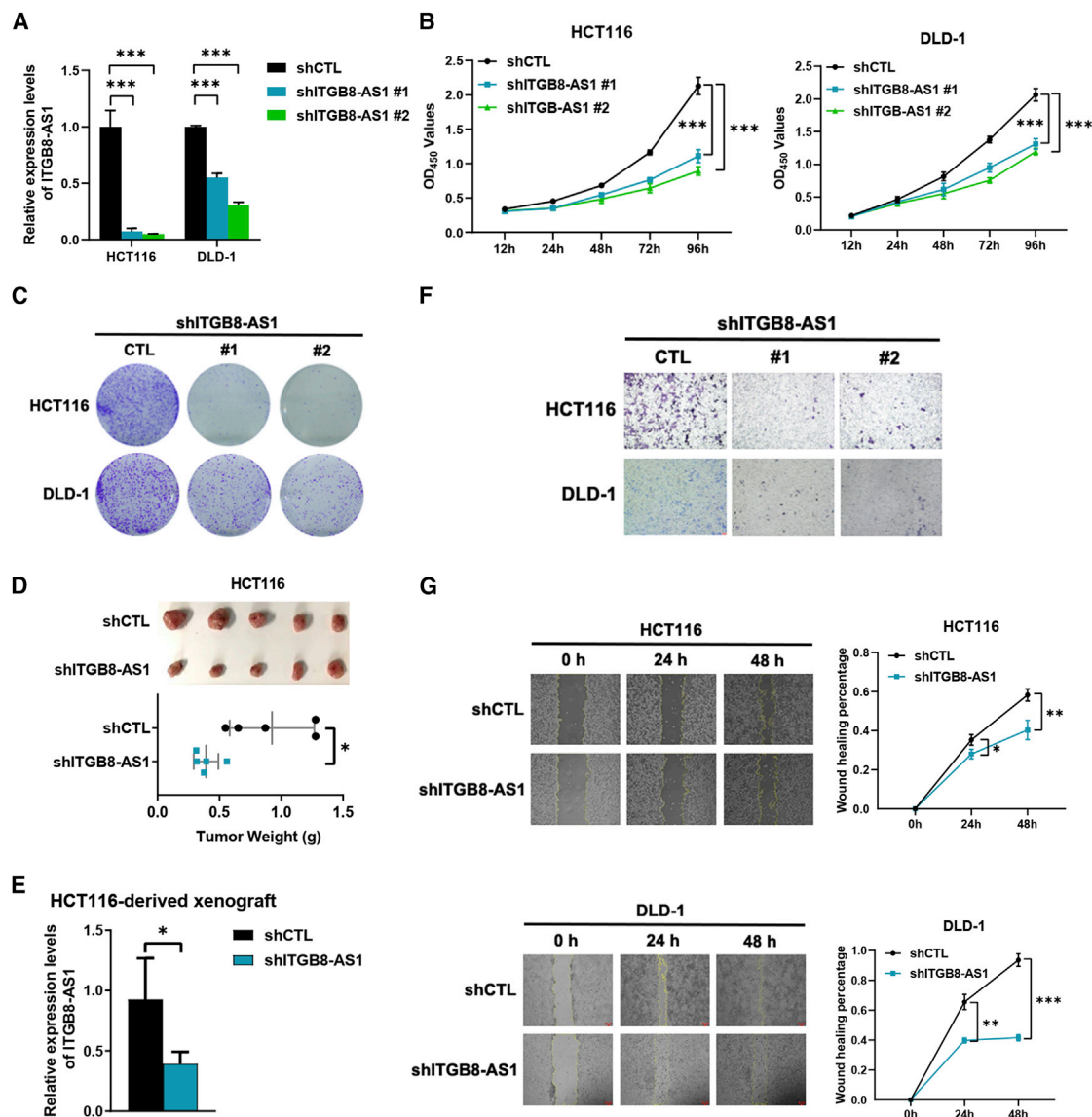


Figure 1. ITGB8-AS1 is required for the growth and migration of CRC

(A) ITGB8-AS1 was knocked down by shRNA in CRC cells. (B) ITGB8-AS1 knockdown reduced cell proliferation in CRC cells. (C) ITGB8-AS1 knockdown impaired colony formation of CRC cells. (D) ITGB8-AS1 knockdown repressed tumor growth of CRC in mice bearing HCT116 cells. (E) ITGB8-AS1 was effectively knocked down *in vivo*. (F and G) ITGB8-AS1 knockdown suppressed migration capabilities in CRC cells. Mean \pm SD. * $p < 0.05$; ** $p < 0.01$; *** $p < 0.001$; by Student's t test.

miRNAs. To create this ceRNA network, LncBase-DIANA v.3.0 and StarBase v.2.0 were harnessed to discover miRNAs interacting with ITGB8-AS1 and target genes of these miRNAs, respectively. Genes annotated in focal adhesion signaling in our work were next overlapped with the above target genes. We focused on key players of focal adhesion signaling, integrins. As presented, four miRNAs, including miR-30c-5p, miR-33b-5p, let-7d-5p, and let-7c-5p, and three target genes, including ITGA3, ITGB3, and ITGA5, were left in the ceRNA network (Figure 5A). With quantitative real-time PCR, knockdown of ITGB8-AS1 was verified to inhibit transcription of ITGA3, ITGA5, and ITGB3 in CRC cells (Figure 5B). Furthermore, downregulation

of ITGA3, ITGA5, and ITGB3 was also observed in xenografts derived from HCT116 cells with ITGB8-AS1 knockdown (Figure S5). Consistently, gain-of-function assays displayed that ITGB8-AS1 overexpression promoted transcription of ITGA3, ITGA5, and ITGB3 in CRC cells (Figure 5C). Moreover, ITGB8-AS1 knockdown could decrease the protein expressions of ITGA3, ITGA5, and ITGB3, while ITGB8-AS1 overexpression increases these protein levels in CRC cells (Figure 5D and 5E).

To further determine which miRNAs are functional in bridging ITGB8-AS1 and integrin genes, we started with rescue assays in HCT116 cells.

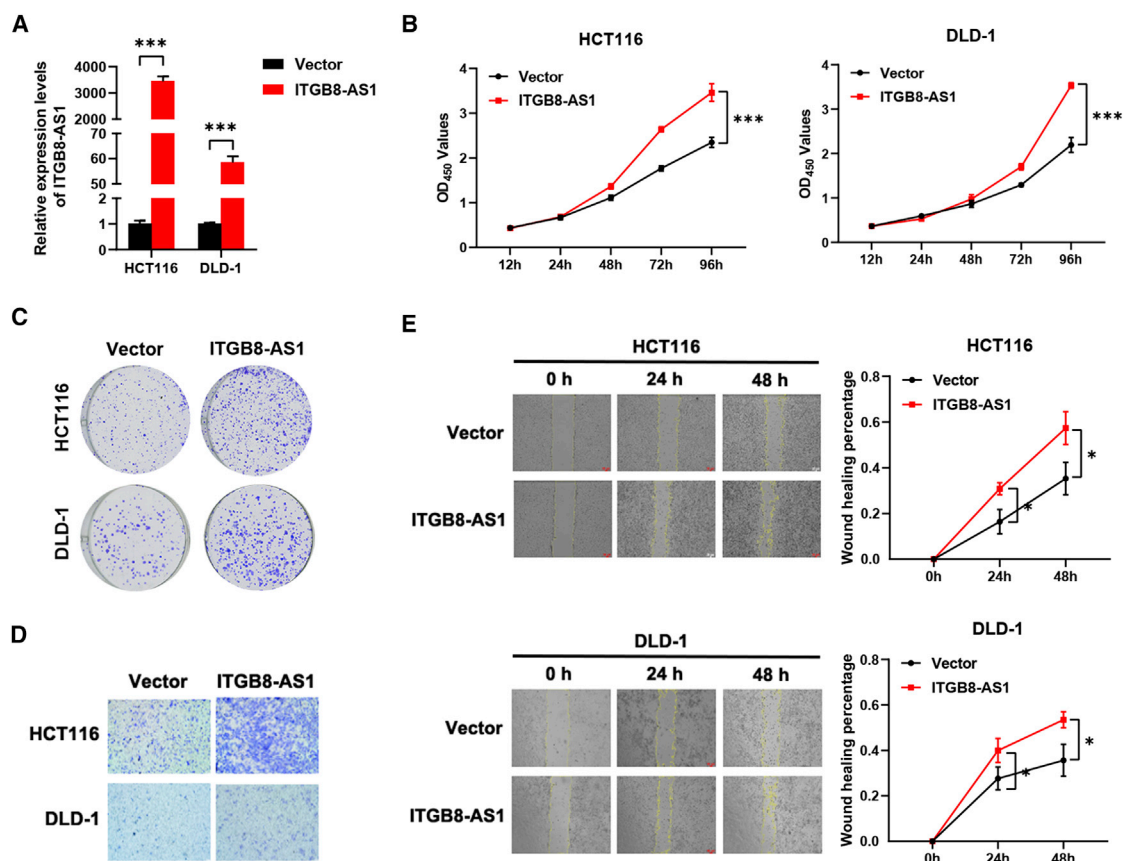


Figure 2. ITGB8-AS1 overexpression enhanced growth and migration of CRC cells

(A) ITGB8-AS1 was overexpressed in CRC cells. (B and C) ITGB8-AS1 overexpression promoted cell viability and colony formation in CRC cells. (D and E) Migration abilities were improved by ITGB8-AS1 overexpression *in vitro*. Mean \pm SD. * $p < 0.05$; ** $p < 0.01$; *** $p < 0.001$; by Student's *t* test.

As presented in Figure 6A, miR-33b-5p inhibitor could rescue the inhibitory effects of ITGB8-AS1 knockdown on ITGA3 transcription. Similarly, let-7c-5p or let-7d-5p was dispensable for ITGB8-AS1-mediated ITGB3 transcription. Instead, miR-30c-5p inhibitor failed to rescue the inhibitory effects of ITGB8-AS1 knockdown on ITGA5 and ITGB3 transcription. Moreover, Ago2 RNA immunoprecipitation (RIP) analysis revealed that ITGB8-AS1 was significantly enriched in Ago2-containing micro-ribonucleoprotein complexes (Figure 6B), suggesting that ITGB8-AS1 directly bound with Ago2 in CRC cells. Dual luciferase reporter assays were then utilized to determine which miRNAs could directly interact with ITGB8-AS1 in HCT116 cells. Co-transfection of the wild-type ITGB8-AS1 vector (Luc-ITGB8-AS1 WT) with miR-33-5p, let-7c-5p, or let-7d-5p mimics rather than miR-30-5p mimics significantly reduced the luciferase activity (Figure 6C). Meanwhile, luciferase activity of the wild-type ITGA3 vector (Luc-ITGA3 WT) was also decreased when miR-33-5p mimics were co-transfected. Similarly, luciferase activity of wild-type ITGB3 vector (Luc-ITGB3 WT) was decreased when let-7c-5p/let-7d-5p mimics were co-transfected (Figure 6D). To further verify whether miR-33b-5p, let-7c-5p, and let-7d-5p could bind to the predicted target sites in ITGB8-AS1, we also constructed mutant ITGB8-AS1 luciferase reporter vectors. As ex-

pected, co-transfection of wild-type ITGB8-AS1 vector (Luc-ITGB8-AS1 WT), but not the mutant ITGB8-AS1 vector (Luc-ITGB8-AS1 MUT for miR-33b-5p, Luc-ITGB8-AS1 MUT2 for let-7c-5p/let-7d-5p; Figure S5), with miR-33b-5p, let-7c-5p, or let-7d-5p mimics displayed significantly reduced luciferase activities in HCT116 cells (Figure 6E). We next examined the binding of ITGA3 with miR-33b-5p, and ITGB3 with let-7c-5p/let-7d-5p, by similar approaches. Luciferase activity was reduced when co-transfecting the wild-type ITGA3 vector (Luc-ITGA3 WT), but not the mutant ITGA3 vector (Luc-ITGA3 MUT), with miR-33-5p mimics (Figure 6E). ITGB3 binding to let-7c-5p/let-7d-5p was similarly validated with wild-type and mutant ITGB3 luciferase reporter vectors (Figure 6E). Taken together, our data suggested that ITGB8-AS1 could sponge miR-33b-5p and let-7c-5p/let-7d-5p to regulate transcription of ITGA3 and ITGB3 in CRC cells, respectively.

ITGB8-AS1 functions as a miRNA sponge for miR-33b-5p and let-7d-5p/let-7d-5p to promote cell proliferation and migration in CRC

To explore whether the oncogenic role of ITGB8-AS1 is linked to its function in sponging miR-33b-5p, let-7d-5p, or let-7d-5p, rescue assays were carried out. Specifically, CCK-8 analysis revealed that miR-33b-5p,

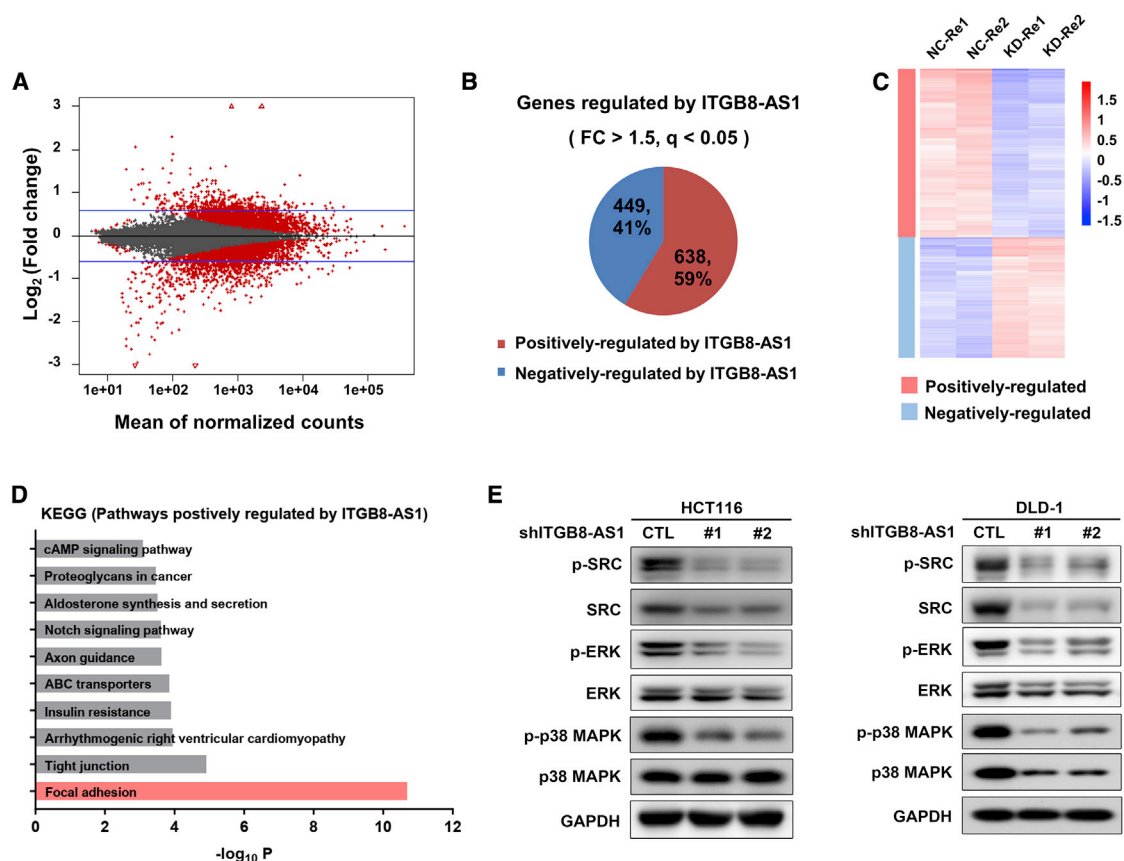


Figure 3. Focal adhesion signaling is positively regulated by ITGB8-AS1 in CRC

(A–C) Gene expression patterns of ITGB8-AS1 knockdown presented by volcano plot, pie plot, and heatmap. NC, negative control; KD, knockdown by siRNA. (D) Top 10 signaling positively regulated by ITGB8-AS1 using KEGG pathway analysis. Red, the most significant cascade. (E) ITGB8-AS1 knockdown decreased phosphorylation levels of focal adhesion signaling proteins.

let-7d-5p, and let-7d-5p inhibitors could all rescue growth inhibition caused by ITGB8-AS1 knockdown in CRC cells (Figure 7A). Suppressive impacts of ITGB8-AS1 knockdown on colony formation were also reversed by miR-33b-5p, let-7d-5p, or let-7d-5p inhibitor in CRC cells (Figure 7B). Moreover, Transwell assays illustrated that miR-33b-5p, let-7d-5p, or let-7d-5p inhibitor could rescue repressive cell migration abilities of CRC cells mediated by ITGB8-AS1 knockdown (Figure 7C). Taken together, ITGB8-AS1 acts as molecular sponge for miR-33b-5p, let-7d-5p, and let-7d-5p, and the functions of ITGB8-AS1 in promoting growth, migration, and focal adhesion signaling were, at least partially, dependent on sponging these miRNAs in CRC.

ITGB8-AS1 served as a potential diagnostic and predictive biomarker for CRC

To examine expression patterns of ITGB8-AS1 in CRC tissues and healthy controls, the GEPIA website tool was employed. Compared to their normal tissues, ITGB8-AS1 was highly expressed both in COAD (colon adenocarcinoma) and READ (rectum adenocarcinoma) samples (Figure 8A). Expression levels of ITGB8-AS1 were also examined in 14 pairs of post-operative CRC tissues and corresponding

para-cancer tissues. Similarly, ITGB8-AS1 expression levels of CRC tissue samples were higher than those of matched normal tissue specimens in our cohort (Figure 8B). To further explore the potential utility of ITGB8-AS1 in CRC liquid biopsy, 7 plasma samples from healthy controls and 7 plasma samples from CRC patients were collected. As exhibited in Figure 8C, CRC patients had higher plasma levels of ITGB8-AS1 than healthy controls, indicating diagnostic values of ITGB8-AS1 in CRC. In another independent cohort, plasma level of ITGB8-AS1 was significantly positively correlated with differentiation ($p = 0.021$; Figure 8D). Stage III and stage IV patients presented higher plasma levels of ITGB8-AS1 than stage I–II patients (Figure 8D). Lymph node involvement was prone to have high ITGB8-AS1 plasma levels despite no statistical significance ($p = 0.07$; Figure 8D). In contrast, neither age, gender, primary tumor location, nor distal metastasis associated with plasma levels of ITGB8-AS1 (Figure 8D). Thus, these data suggested that high plasma levels of ITGB8-AS1 could serve as a diagnostic and predictive biomarker for CRC. We also assessed correlations between ITGB8-AS1 expressions and its target genes. As revealed in Figure 8E, plasma level of ITGB8-AS1 was closely related to that of ITGA3 and ITGB3 in CRC patients, with Pearson's correlation coefficient (r) up to 0.85 and 0.84, respectively.

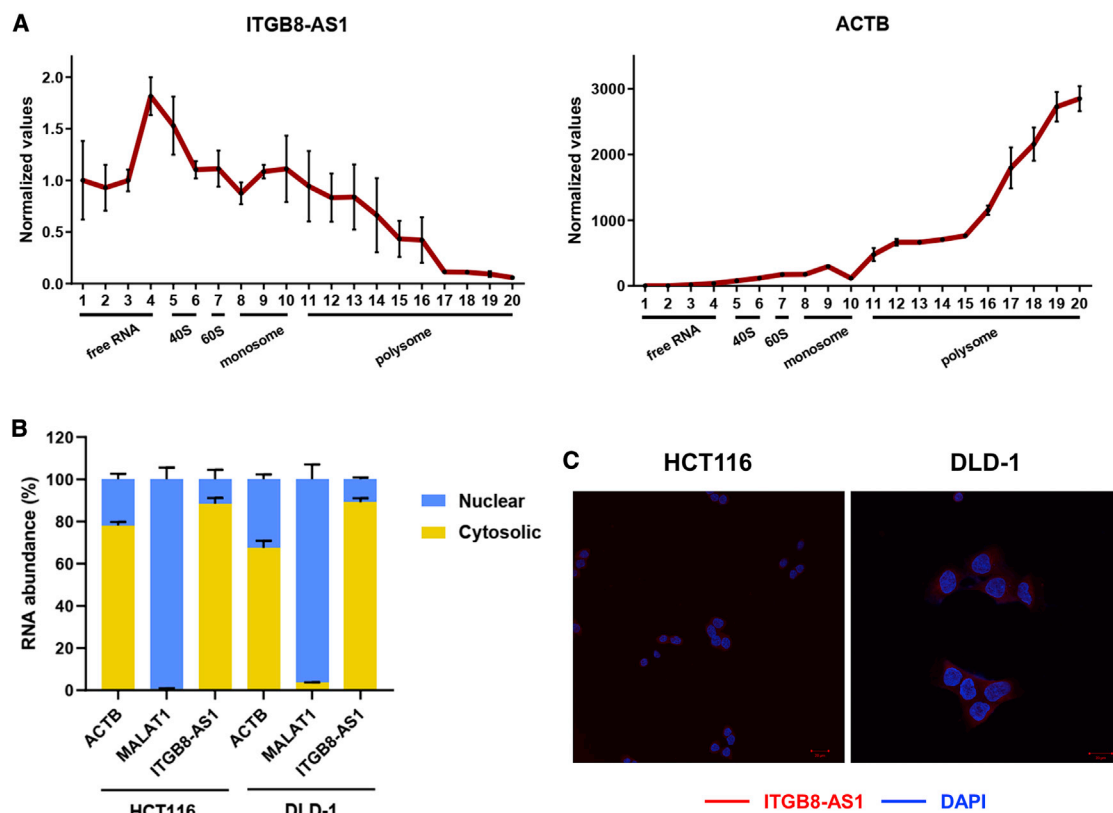


Figure 4. Coding potential and subcellular localization analysis of ITGB8-AS1 in CRC cells

(A) Distribution of ITGB8-AS1 and ACTB in free RNA, monosome, and polysome fractions analyzed by quantitative real-time PCR in HCT116 cells. (B and C) Subcellular localization analysis of ITGB8-AS1 with cellular fractionation and RNA-FISH method in CRC cells. Red, ITGB8-AS1. Blue, DAPI.

ITGB8-AS1 serve as a potential therapeutic target against CRC

As mentioned above, ITGB8-AS1 promoted malignant behaviors and was upregulated in CRC, which gave a rationale for therapeutic targeting of this lncRNA. To explore therapeutic potentials of ITGB8-AS1 inhibition, antisense oligonucleotide (ASO) targeting ITGB8-AS1 was applied in various CRC preclinical models including patient-derived xenograft (PDX). Knockdown efficiency of ITGB8-AS1-ASO in CRC cells is presented in Figure 9A. CCK-8 and colony-formation analysis demonstrated that ITGB8-AS1-ASO markedly suppressed cell viability and colony formation in CRC cells (Figures 9B and 9C). To test *in vivo* anti-growth activity of targeting ITGB8-AS1, HCT116-derived xenograft and PDX models were utilized. It was found that ITGB8-AS1-ASO exerted anti-tumor efficacy both in mice bearing HCT116 cells and the CRC PDX model (Figures 9D and 9E). To evaluate impacts of targeting ITGB8-AS1 on liver metastasis in CRC, we used a cell model derived from CRC-LM PDXs that were established by liver metastasis specimens from CRC patients, called the CRC-LM PDX-derived cell model, that is a CRC-LM PDC model (LIDE Biotech, Shanghai, China). As revealed, ASO targeting ITGB8-AS1 could inhibit growth in CRC-LM PDC models (Figure 9F). Moreover, all miR-33b-5p, let-7c-5p, and let-7d-5p inhibitors could mitigate anti-cancer effects of ASO targeting ITGB8-AS1 in the CRC-LM PDC model (Figure 9G).

Thereby, ITGB8-AS1 could serve as a novel therapeutic target against CRC, and ASO targeting ITGB8-AS1 seemed to be a promising strategy in the treatment of CRC patients, including those with liver metastasis.

DISCUSSION

Thousands of lncRNAs identified by transcriptomic analysis are involved in human disease, many of which have been shown to play critical roles in almost every step of cancer development, such as proliferation, migration, and invasion.^{3,4} Nevertheless, the majority of these lncRNAs still remain functionally uncharacterized. Our previous work screened differentially expressed lncRNAs by comparing CRC tissues and paired normal tissues, among which the unstudied ITGB8-AS1 was highly expressed in CRC.²⁸ With loss- and gain-of-function experiments, the present study elucidated that ITGB8-AS1 was dispensable for CRC cell proliferation and tumor growth along with migration. Transcriptomics analysis highlighted focal adhesion signaling as ITGB8-AS1-regulated downstream cascades. Given ITGB8-AS1 predominantly localized in the cytosol, we further unveiled that ITGB8-AS1 sponged miR-33b-5p and let-7c-5p/let-7d-5p to regulate transcription of ITGA3 and ITGB3, respectively. ITGB8-AS1 clinical relevance was underscored by its high expression in CRC tissues and plasma, and high plasma levels of ITGB8-AS1

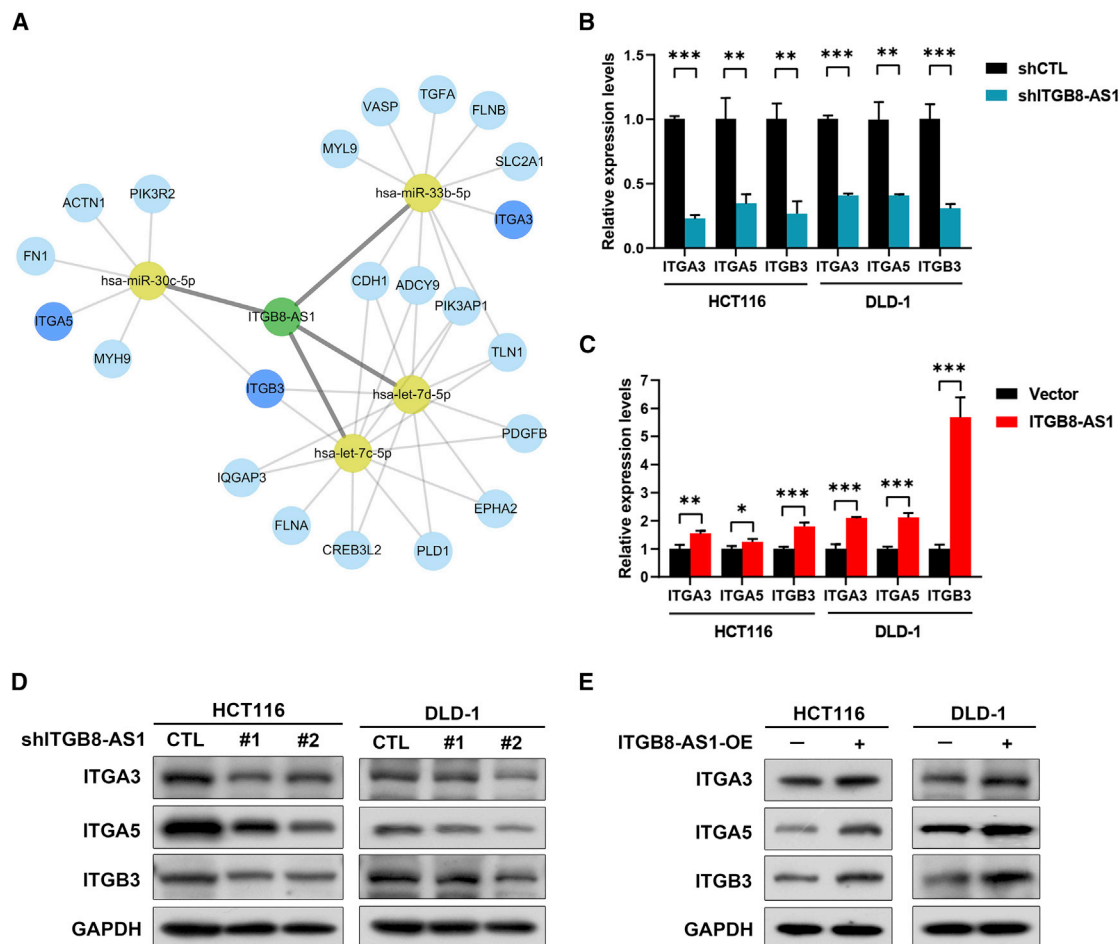


Figure 5. ITGB8-AS1 sponges miRNAs to regulate the expression of integrins

(A) ceRNA network of ITGB8-AS1/miRNAs/target genes overlapped with focal adhesion signaling components annotated in our RNA-seq data. (B) ITGB8-AS1 knockdown reduced expression levels of integrin family members in CRC cells. (C) ITGB8-AS1 overexpression transcriptionally increased integrin family members. (D) ITGB8-AS1 knockdown inhibited protein expressions of integrin family members in CRC cells. (E) ITGB8-AS1 overexpression increased protein levels of integrin family members in CRC cells. Mean \pm SD. * $p < 0.05$; ** $p < 0.01$; *** $p < 0.001$; by Student's *t* test.

predicted poor differentiation and advanced TNM stage. In addition, targeting ITGB8-AS1 using ASO yielded markable anti-tumor response in CRC pre-clinical models, including PDX and CRC-LM PDC (Figure 10).

Focal adhesion is integrin-mediated cell-ECM linkages, behaving as both a physical anchor and a signaling hub in response to biochemical components and mechanical tension. The focal adhesion pathway is initiated by integrin activation, resulting in cascade activation of FAK, SRC, and downstream components such as ERK and p38 MAPK.²⁴ Integrin-centered focal adhesion signaling contributes to almost every aspect of cancer cell activity.^{25,26} However, tumor-relevant lncRNAs targeting integrin-mediated focal adhesion signaling in CRC remain largely unknown. Our study demonstrated that an uninvestigated lncRNA, ITGB8-AS1, promoted CRC cell proliferation, tumor growth, and migration through focal adhesion signaling (Figures

1–3). Regarding how lncRNAs link focal adhesion to cancer, the majority of previous studies were dedicated to lncRNA-associated integrin transcription activity, represented by ITGA5, ITGA6, ITGB1, and ITGB3, and integrin downstream pathways.^{29–39} ITGA3 and ITGB3 were target genes of ITGB8-AS1 in our study (Figure 5). Moreover, ITGB8-AS1 knockdown attenuated integrin downstream pathways, including phosphorylation of SRC, ERK, and p38 MAPK (Figure 3E).

Subcellular localization of lncRNA is a determinant of its mode of action. Cytoplasm-enriched lncRNAs typically modulate expression of specific mRNAs at the posttranscriptional level by interacting with miRNAs or RNA-binding proteins. In this study, we found that ITGB8-AS1 acted as a ceRNA to regulate transcription of ITGA3 and ITGB3 by sponging miR-33b-5p and let-7c-5p/let-7d-5p, respectively (Figures 5 and 6). Consistent with the established

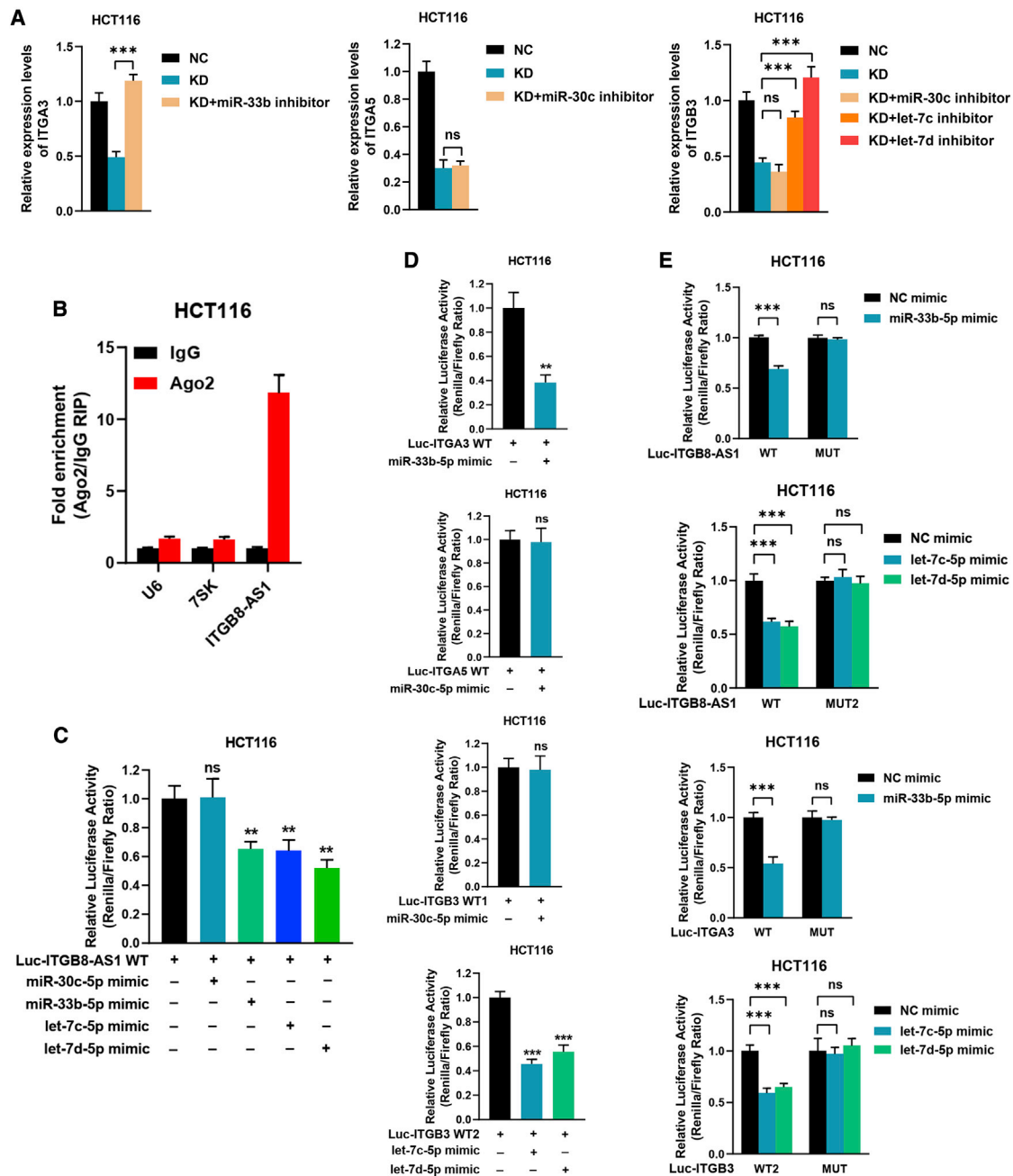


Figure 6. Validation of ceRNA network of ITGB8-AS1/miRNA/integrins

(A) Effects of co-transfecting shITGB8-AS1 with miRNA (miR-30c, miR-33b, let-7c, or let-7d) inhibitors on target gene (ITGA3, ITGA5, or ITGB3) expressions in HCT116 cells. (B) Ago2 RIP was performed to assess endogenous Ago2 binding to RNA; IgG was used as the control. The levels of ITGB8-AS1, miR-30c, miR-33b, let-7c, and let-7d were determined by quantitative real-time PCR and presented as fold enrichment in Ago2 relative to input. (C and D) Dual-luciferase reporter assays were conducted with wild-type luciferase report vectors to screen potential ITGB8-AS1/miRNA/integrin axes. (E) Dual-luciferase reporter assays were conducted with wild-type and mutated (putative binding sites for miR-33b, let-7c, and let-7d were mutated) luciferase report vectors to validate screened ITGB8-AS1/miRNA/integrin axes. NC, negative control; KD, knockdown by shRNA. Mean \pm SD. * $p < 0.05$; ** $p < 0.01$; *** $p < 0.001$; by Student's *t* test.

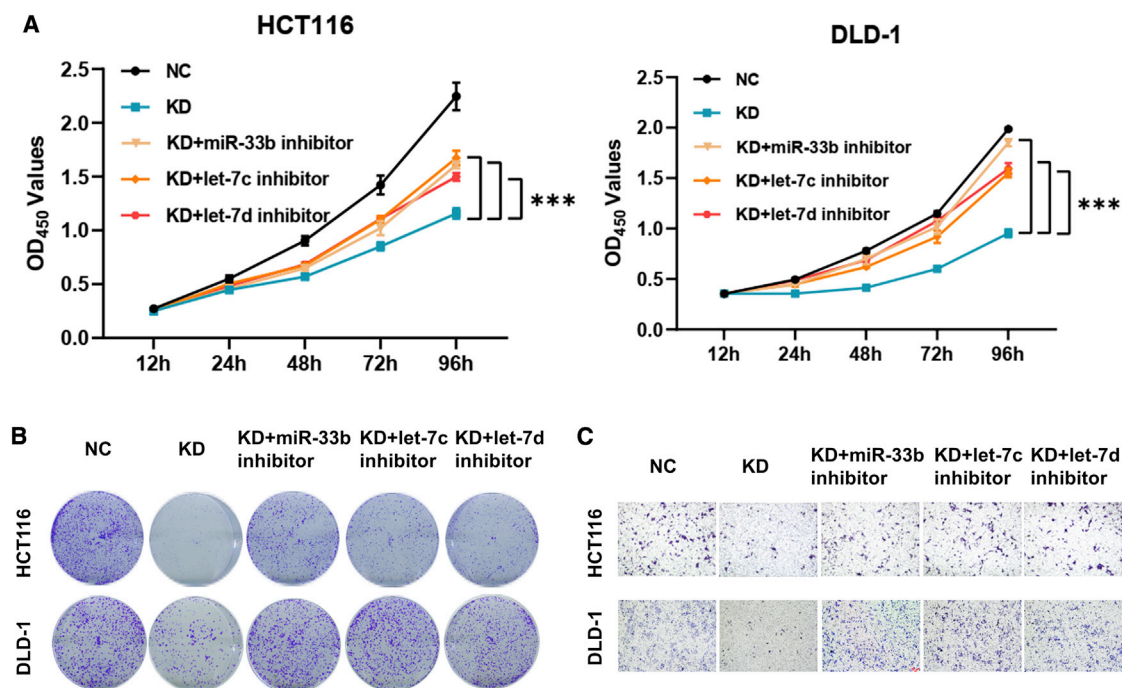


Figure 7. ITGB8-AS1 sponges miR-33b-5p and let-7c-5p/let-7d-5p to promote growth and migration in CRC

(A–C) Co-transfection with miRNA (miR-33b, let-7c, or let-7d) inhibitors mitigated inhibitory effects of ITGB8-AS1 knockdown on cell proliferation, colony formation, and migration in CRC cells. NC, negative control; KD, knockdown by shRNA. *** $p < 0.001$; by Student's *t* test.

ceRNA network, monotherapy of all miRNA inhibitors (miR-33b-5p, let-7c-5p, and let-7d-5p) promoted growth and migration (Figure S6) and increased protein levels of their corresponding target genes, ITGA3 and ITGB3, respectively (Figure S7). In parallel to preclinical data, plasma levels of ITGB8-AS1 highly correlated with those of its target genes, ITGA3 and ITGB3 (Figure 8E). Previous studies revealed that lncRNA-activated ITGB3 transcription entailed miRNA sponge (for instance, miR-590-3p/miR-1275/miR-30a-5p).^{40,41} In CRC, nuclear lncRNA HOXD-AS1 suppressed ITGB3 transcription and integrin downstream pathways via the neighborhood gene HOXD3.¹⁴ Instead, lncRNA-affected ITGA3 expression was almost uninvestigated expect for an *in vitro* observation that the lncRNA NEAT1/miR-339-5p/ITGA3 axis was required for tongue cancer.⁴² Other studies show that ITGA5 is transcriptionally regulated by several cancer-associated lncRNAs,^{31,32,43} and ITGA5 also acted as a target gene of ITGB8-AS1 in the present research (Figure 5). However, the predicted miR-30c-5p sponging seemed not to be the mechanism (Figure 6). Mechanisms underlying how ITGB8-AS1 regulated ITGA5 expression remained undeciphered.

Recently, more and more lncRNA levels in CRC tissues have been verified to positively or negatively correlate with patients' clinicopathological parameters or survival, such as SNHG6, LINRIS, FEZF1-AS1, RP11, GLCC1, OLA1P2, HOXD-AS1, SATB2-AS1, and ZNF1-AS1.^{6–8,11,14,18,44–46} Emerging evidence has displayed clinical relevance of circulating lncRNAs in CRC, highlighting diagnostic or prognostic values of altered lncRNA plasma levels, such as CCAT1,

CCAT2, HOTAIR, HOTAIRM1, UCA1, TUG1, MALAT1, GAS5, XIST, 91H, PVT1, NEAT1, CRNDE, HOXA-AS2, SLC25A25-AS1, RPPH1, and HOTTIP.^{47–49} Among them, UCA1, TUG1, GAS5, 91H, CRNDE, HOXA-AS2, RPPH1, and HOTTIP are also detected and dysregulated in exosomes. Of interest, circulating lncRNAs (for instance, SNHG11, CCAT1, and UCA1) serve as novel biomarkers for early detection of CRC, as they distinguished pre-cancerous lesions (colorectal polyps and adenomas) well from healthy controls and early-stage CRC.^{47,50} Moreover, certain lncRNA plasma levels in CRC (such as ATB, FER1L4, ZFAS1, SNHG11, LINC00909, and LINC00654) can be altered after surgical resection, suggesting their promising applications for dynamically monitoring tumor burdens and clinical outcomes.^{47,50} In our work, ITGB8-AS1 level in CRC plasma was higher than in normal plasma, and elevated plasma level of ITGB8-AS1 was associated with poor differentiation and TNM stage (Figure 8). The findings indicated circulating ITGB8-AS1 as a novel diagnostic and prognostic biomarker for CRC. Studies in a larger cohort and/or exosomal ITGB8-AS1 will facilitate future potential clinical utility of circulating ITGB8-AS1 in CRC.

ASO-based strategy that reduces transcripts of lncRNAs via RNase H-dependent degradation in the nucleus is a representative of lncRNA-directed therapies and is under active investigation.⁵¹ ASO against certain lncRNAs is more and more prevalently harnessed to assess therapeutic efficacy of targeting lncRNA or augmented effectiveness of targeting lncRNA-combined regimens.^{52–55} In the present study, ASO targeting ITGB8-AS1 achieved marked anti-tumor

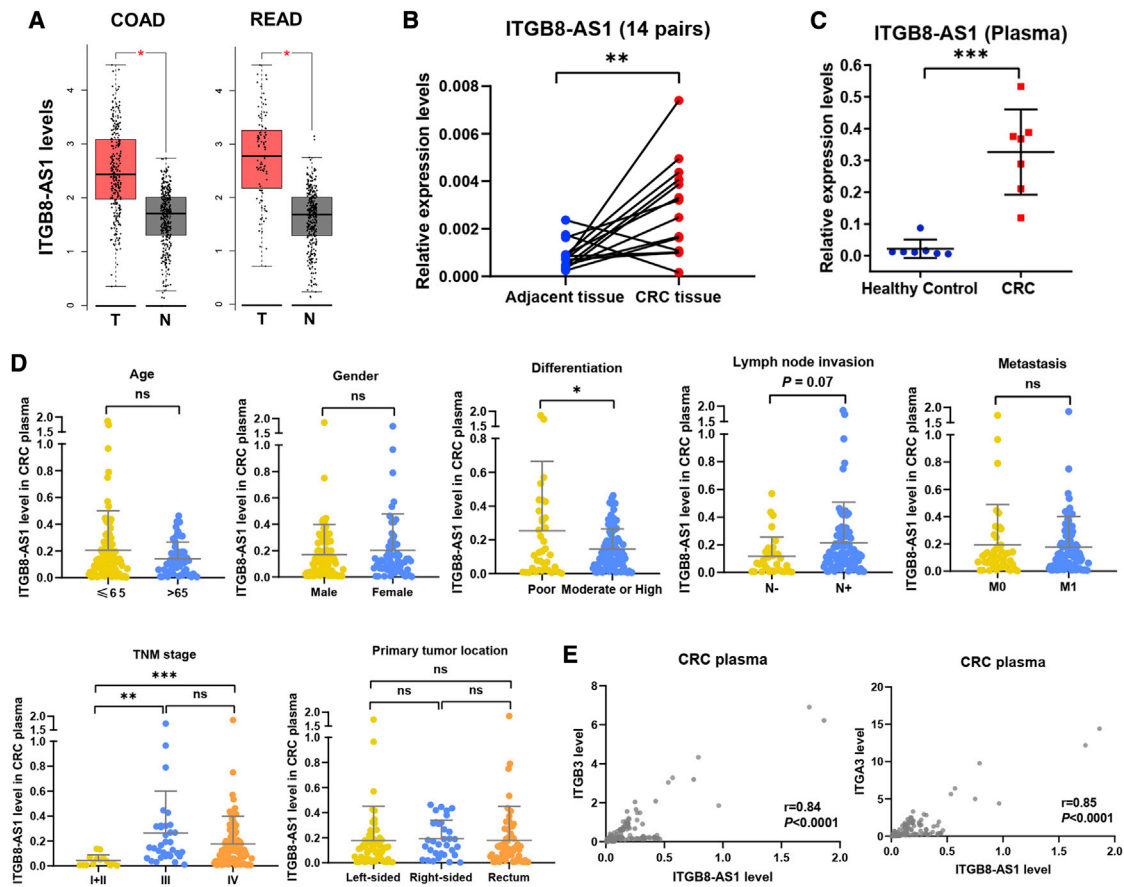


Figure 8. ITGB8-AS1 served as a potential biomarker for CRC

(A) Expression level of ITGB8-AS1 was higher than that of healthy controls in COAD (colon adenocarcinoma) and READ (rectum adenocarcinoma) analyzed with GEPIA web tools. T, tumor; N, normal. (B) Statistical analysis of ITGB8-AS1 expression in our cohort of 14 pairs of CRC and adjacent normal tissues. (C) ITGB8-AS1 plasma level in our cohort of CRC patients was elevated compared to those of healthy controls. (D) Predictive value of ITGB8-AS1 plasma level in clinical pathological features using a CRC cohort ($n = 150$). (E) Plasma level of ITGB8-AS1 was closely correlated with that of ITGA3 and ITGB3 in a CRC cohort ($n = 150$). Pearson correlation analysis. Mean \pm SD. * $p < 0.05$; ** $p < 0.01$; *** $p < 0.001$; ns, not significant; by Student's *t* test, paired *t* test or ANOVA.

responses in several CRC preclinical models, including cell lines and their derived xenografts as well as PDX (Figure 9). Of note, liver metastasis was also inhibited by ASO targeting ITGB8-AS1, as indicated by the CRC-LM PDC model, the PDX-derived cell model whose PDX was established by liver metastasis specimens from CRC patients (Figure 9). Thereby, ITGB8-AS1 can serve as a promising therapeutic target against CRC. Moreover, how ITGB8-AS1 is highly expressed in CRC remains unclear. As known, gene overexpression can result from various genetic alterations, copy number gain and gene amplification included. To give some insight into this issue, we retrieved cBioPortal website tools. Out of 592 CRC patients involved, the copy number of ITGB8-AS1 was increased in 344 patients, and the ITGB8-AS1 gene was amplified in 2 patients (Figure S8).

Taken together, we elucidated biological functions and clinical significance of a cytoplasmic lncRNA, ITGB8-AS1, in CRC. As a molecular sponge to regulate ITGA3 and ITGB3, ITGB8-AS1 promoted CRC growth and migration through integrin-mediated focal adhesion

signaling. ITGB8-AS1 expression was upregulated in CRC cells, tissues, and plasma. Targeting ITGB8-AS1 elicited marked anti-tumor efficacy in CRC preclinical models. Elevated ITGB8-AS1 in CRC plasma predicted poor differentiation and advanced TNM stage. These data suggest ITGB8-AS1 could serve as a promising biomarker and novel therapeutic target of CRC.

MATERIALS AND METHODS

Reagents and antibodies

Clinical specimens

Histopathologically confirmed CRC specimens and matched normal tissues from post-operative patients, along with plasma of CRC patients and healthy controls were collected as described in our previous study, which was approved by the ethics committee of the Affiliated Nanhua Hospital, University of South China.²⁸ Plasma from patients with CRC in another cohort ($n = 150$) was obtained with written informed consent at the First Affiliated Hospital of Xiamen University (Xiamen, China). The study protocol was approved by the ethics

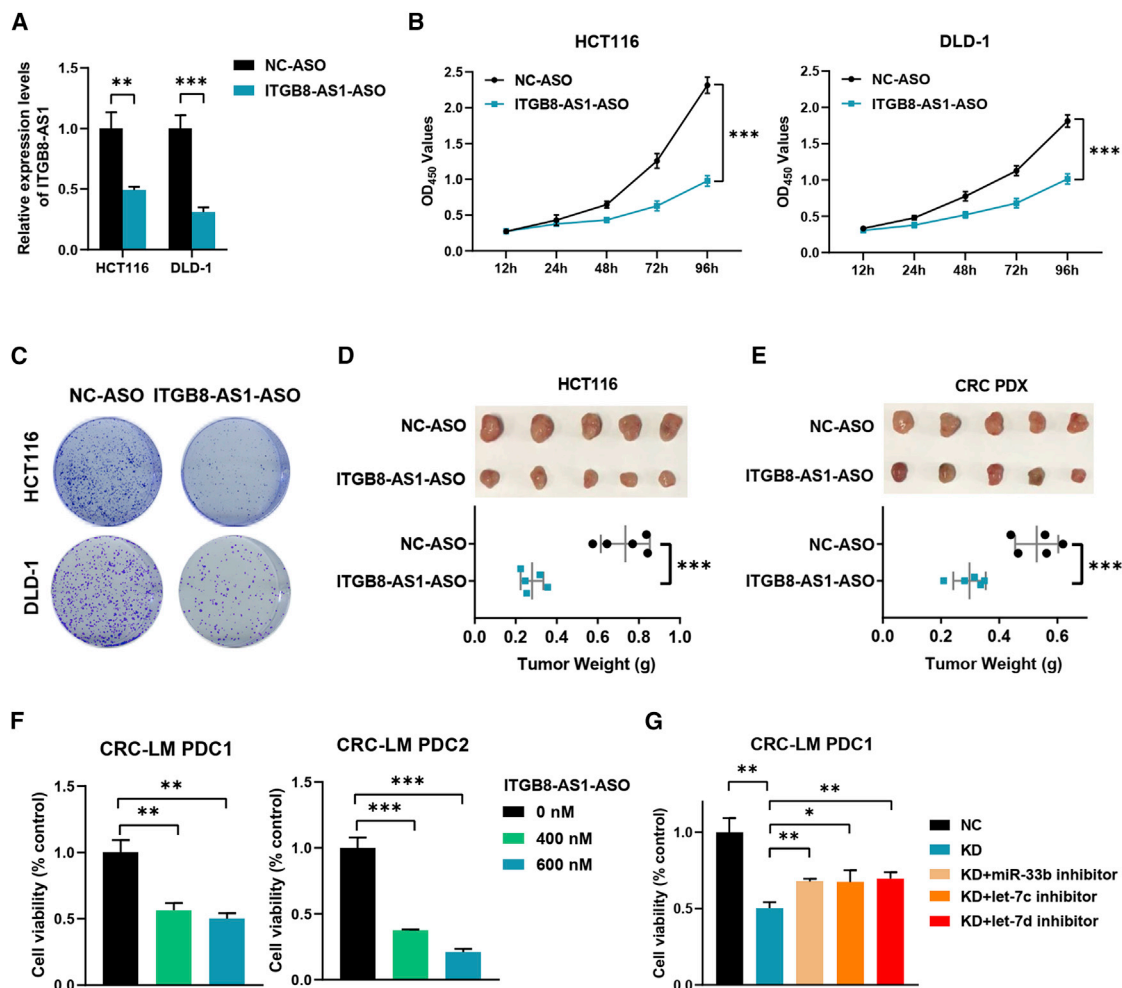


Figure 9. ITGB8-AS1 serves as a potential therapeutic target in CRC

(A) ASO targeting ITGB8-AS1 effectively reduced expressions of ITGB8-AS1 in CRC cells. (B and C) Targeting ITGB8-AS1 with ASO suppressed cell proliferation and colony formation in CRC cells. (D and E) ITGB8-AS1 blockade using ASO elicited anti-tumor efficacy both in HCT116-derived xenograft and CRC PDX model. (F) ITGB8-AS1-ASO inhibited liver metastasis revealed by CRC-LM PDC models. CRC-LM PDC, CRC-LM PDX-derived cell; CRC-LM PDX, PDX established by liver metastasis specimens from CRC patients. (G) Co-treatment with miRNA (miR-33b, let-7c, or let-7d) inhibitors mitigated inhibitory effects of ITGB8-AS1 blockade by ASO on cell viability of CRC-LM PDC model. NC, negative control; KD, knockdown by ASO (600 nM). Mean \pm SD. * $p < 0.05$; ** $p < 0.01$; *** $p < 0.001$; by Student's *t* test.

committee of the First Affiliated Hospital of Xiamen University. The research was carried out in accordance with the provisions of the Declaration of Helsinki. All tissue specimens were immediately frozen in liquid nitrogen and stored at -80°C until used. Peripheral whole-blood samples were collected in EDTA anticoagulation tubes, immediately centrifuged at 3,000 rpm for 8 min to separate plasma, and stored at -80°C until used.

Cell lines and cell culture

The human CRC cell lines HCT116, DLD-1, SW620, SW480, CaCO-2, HT-29, and RKO, and normal colon epithelial cell line ccc-HIE-2 were purchased from the Cell Bank of Chinese Academy of Sciences (Beijing, China). HCT116 and HT-29 were cultured in McCoy's 5A medium, DLD-1 in PRMI 1640 medium, SW620 and

SW480 in L15 medium, CaCO-2 in MEM medium, and RKO and ccc-HIE-2 in Dulbecco's modified Eagle's medium. All the media were supplemented with 10% fetal bovine serum (Biological Industries) and 1% penicillin and streptomycin (HyClone, Logan, UT, USA). All the cell lines were cultured at 37°C with 5% CO_2 .

Gene knockdown and overexpression

ITGB8-AS1 siRNA and ASO were purchased from RiboBio (Guangzhou, China). ITGB8-AS1 shRNAs were cloned into Lenti-viral pLKO.1 vector between Age and EcoRI restriction enzyme sites, followed by vector packaging as described in a previous study.²⁸ Plasmid overexpressing ITGB8-AS1 was obtained from Mailgene (Beijing, China). All sequence information is presented in Table S2.

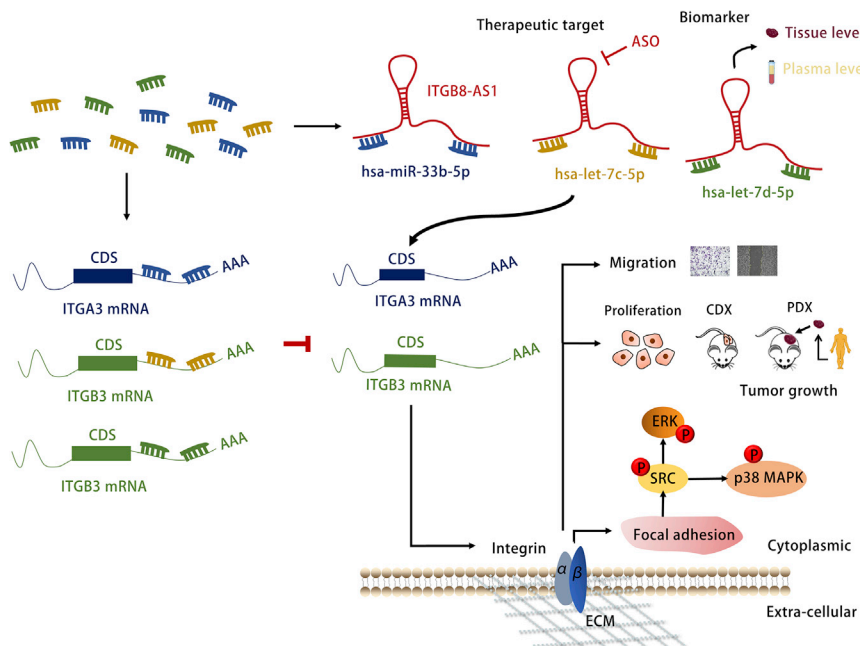


Figure 10. Schematic depicting ITGB8-AS1-activated integrin adhesion and growth in CRC

ITGB8-AS1 sponged miR-33b-5p to regulate expressions of ITGA3 as well as let-7c-5p and let-7d-5p to regulate expressions of ITGB3, followed by an activation of integrin-mediated focal adhesion signaling. ITGB8-AS1 could serve as a novel therapeutic target and circulating biomarker for patients with CRC.

RNA-FISH

RNA-FISH experiments were performed according to manufacturer's protocol from RiboBio (Guangzhou, China). Briefly, CRC cells were planted into a 35 mm glass-bottom dish (NEST, Jiangsu, China) and incubated overnight in complete medium. Cells were fixed with 4% paraformaldehyde (Solarbio, Beijing, China) for 10 min at room temperature, permeabilized with 0.5% Triton X-100 (Amresco) for 5 min at 4°C, and blocked with pre-hybridization buffer (ZSJB-BIO, Beijing, China) for 30 min at 37°C. Cells were incubated with 40 nM FISH probes of ITGB8-AS1 overnight

at 37°C in the dark (RiboBio, Guangzhou, China), followed by washing with hybridization washing buffer I (4 × SSC, 0.1% Tween-20), hybridization washing buffer II (2 × SSC), and hybridization washing buffer III (1 × SSC) in order at 42°C in the dark. Nuclei were counterstained with DAPI (0.1 g/mL). Following PBS washing three times, images were captured using a Carl Zeiss laser confocal microscope. ITGB8-AS1 subcellular localization was indicated by the distribution of red signals.

CRC cells were transfected with plasmids, siRNA, or ASO by Lipofectamine 3000 (Thermo Fisher Scientific) according to the manufacturer's instructions for subsequent *in vitro* experiments. HCT116 cells were infected with lentiviral construct of ITGB8-AS1 shRNA and its control vector and cultured in selective medium containing 2 µg/mL puromycin (Invitrogen, Thermo Fisher Scientific) for about 2–4 weeks to establish stably infected cell lines used in *in vivo* experiments.

Cell proliferation, colony formation, and migration assays

Following transfection, cell viability was measured using a CCK-8 commercial kit (Dojindo, Tokyo, Japan) according to the manufacturer's protocol. Absorbance was measured at 450 nm using a spectrophotometer. Colony formation, Transwell, and wound-healing assays were performed according to previously described methods.²⁸

Subcellular fractionation

The experiment was performed according to a previous protocol.⁵⁶ Following scrapping and centrifuging, CRC cell pellets were incubated for 15 min to swell in ice-cold membrane lysis buffer (10 mM [pH 8.0] HEPES, 1.5 mM MgCl₂, 10 mM KCl, 1 mM DTT, with protease and RNase inhibitors). After adding 1% NP-40 and vortex, cytoplasmic fraction was collected by 3-min centrifugation at maximum speed (15,000 rpm). Sediments were then rotated vigorously at 4°C for 30 min in nuclear envelope lysis buffer (20 mM [pH 8.0] HEPES, 1.5 mM MgCl₂, 25% glycerol, 420 mM NaCl, 0.2 mM EDTA, 1 mM DTT with protease and RNase inhibitors). Nuclear fraction was collected by 15-min centrifugation at maximum speed. Both cytoplasmic and nuclear RNAs were extracted using Trizol methods for quantitative real-time PCR.

Isolation of ribosome-associated RNAs

Ribosomal fractions were obtained as described.⁵⁷ In brief, HCT116 cells were treated with cycloheximide (0.1 mg/mL) to fix ribosomes on RNAs and then lysed in hypotonic buffer (5 mM [pH 7.5] Tris-HCl, 2.5 mM MgCl₂, 1.5 mM KCl) supplemented with 0.1 mg/mL cycloheximide, 2 mM DTT, protease and RNase inhibitor, 0.5% Triton X-100, and 0.5% sodium deoxycholate. Polysomes were isolated by centrifugation at 15,000 rpm for 5 min at 4°C, and 10% lysates were kept as an input. The remanent lysates were loaded on a 10%–50% sucrose gradient and centrifuged at 100,000 × g for 4 h at 4°C. Fractions were collected using a programmable gradient fractionator (Isco), and the absorbance at 254 nm was measured. RNAs in collected fractions were extracted with Trizol and detected by quantitative real-time PCR to analyze distribution of ITGB8-AS1 and ACTB in free RNA, monosome, and polysome.

RNA-seq and data analysis

After siRNA transfection for 48 h, ITGB8-AS1-knockdown HCT116 cells and their controls were collected for RNA-seq. Total RNA was isolated by the Trizol method with removal of genomic DNA using DNase I. RNA integrity was confirmed with an Agilent 2100

Bioanalyzer (Agilent Technologies). Next-generation sequencing was performed by an Illumina HiSeq instrument according to the manufacturer's instructions (Illumina, San Diego, CA, USA). Sequences were processed and analyzed by Amogene (Xiamen, China). RNA-seq data were deposited in the Gene Expression Omnibus database.

Quantitative real-time PCR

Total RNA from cells, tissues, and plasma was extracted using RNAiso Plus or RNAiso Blood (Takara) following the manufacturer's protocol. First-strand cDNA synthesis from total RNA was carried out using All-In-One RT MasterMix (Abm), followed by quantitative PCR using AriaMx quantitative real-time PCR machine (Agilent Technologies). The amplified transcript level of each specific gene was normalized to ACTB. Primer sequence information is presented in Table S3.

Western blotting

After treatment, CRC cells were scrapped and lysed using a CytoBuster protein extraction reagent (Merck Millipore) in the presence of protease and phosphatase inhibitor cocktail tablets (Roche, Basel, Switzerland). Protein concentration was measured with a BCA Protein Assay Kit (Applygen, Beijing, China). Soluble lysates were subjected to SDS-PAGE and transferred to polyvinylidene fluoride (PVDF) membranes (Merck Millipore). After blocking with 5% BSA (BioFroxx, Germany) or fat-free milk, membranes were probed with primary antibodies at 4°C overnight and secondary anti-rabbit or anti-mouse antibodies at room temperature for 1 h. Signals were visualized after incubation with Clarity Western ECL substrate (Bio-Rad, Hercules, CA, USA). All antibodies were purchased from Cell Signal Technology (CST, Danvers, MA, USA), including primary antibodies against p-SRC (#6943), p-ERK (#4370), p-p38 MAPK (#4511), SRC (#2109), ERK (#4695), p38 MAPK (#8690), and GAPDH (#5174), as well as secondary anti-rabbit (#7074) and anti-mouse (#7076) antibodies.

Ago2 RIP

Ago2 RIP was performed as described previously. Briefly, cells transfected with 3× FLAG-tagged AGO2 plasmid were lysed in polysome lysis buffer that consisted of 100 mM KCl, 5 mM MgCl₂, 10 mM HEPES (pH 7.0), 0.5% NP-40, 1 mM DTT, 100 U/mL RNasin RNase inhibitor (Promega), 2 mM vanadyl ribonucleoside complexes solution (Sigma), and 25 μL/mL protease inhibitor cocktail (Sigma). Supernatants were collected by centrifugation, part of which was reversed as an input. After an incubation with antibodies against FLAG or IgG, lysates were subjected to immunoprecipitation by using anti-FLAG M2 agarose (Sigma) followed by washing with polysome lysis buffer four times and polysome lysis buffer plus 1 M urea four times. RNAs were released by adding 150 μL of polysome lysis buffer with 0.1% SDS and 45 μg proteinase K (Ambion) and incubated at 50°C for 30 min.

Luciferase reporter assay

Full-length ITGB8-AS1 and its mutant forms, together with 3' UTR of target genes and their mutant forms, all of which included wild-type

or mutated putative miRNA (miR-30c-5p, miR-33b-5p, let-7c-5p, and let-7d-5p) binding sites, were cloned into psiCHECK2 vector with NotI and XhoI restriction enzymes (Promega). Information on binding sites used in plasmid construction is presented in Figure S9.

HCT116 cells were seeded into 96-well plates and allowed to adhere overnight. The cells were then co-transfected with a mixture of wild-type/mutant-type luciferase vectors and control/miRNA mimics as listed in Figures 4C–4E for 36 h. Luciferase activity was measured with a Dual-Luciferase Assay System (Promega) by Spark Multimode Microplate Reader (Tecan, Switzerland).

Animal experiments

To test effects of ITGB8-AS1 knockdown on tumor growth, HCT116 cells stably expressing shITGB8-AS1 and their control shCTL were detached with trypsin/EDTA (Gibco) and re-suspended with PBS to a final concentration of 1×10^8 cells/mL. Then 100 μL cell suspension was inoculated subcutaneously in the right flank of approximately 6-week-old female BALB/c nude mice (n = 5 for each group; Vital River Laboratories, Beijing, China). All mice were sacrificed 20 days after subcutaneous inoculation. To evaluate the therapeutic potential of targeting ITGB8-AS1 with ASO, BALB/c nude mice were subcutaneously implanted with HCT116 cells and CRC PDXs. When tumor volume reached approximately 100–200 mm³, mice bearing HCT116 cells or CRC PDX were randomly assigned to NC-ASO and ITGB8-AS1-ASO groups (n = 5 in each group). NC-ASO and ITGB8-AS1-ASO (10 nM each tumor) were given by intra-tumoral injection every 3 days for 21 days. After the final administration, all mice were sacrificed. Tumors were then stripped and weighed. Mice were housed under specific pathogen-free conditions in the Xiamen University Laboratory Animal Center. All animal experiments were approved by the Xiamen Animal Care and Use Committee and complied with the internationally recognized ARRIVE guidelines (Animal Research: Reporting of *In Vivo* Experiments).

To evaluate impacts of targeting ITGB8-AS1 on liver metastasis in CRC, we used a cell model derived from CRC-LM PDXs that were established by liver metastasis specimens from CRC patients, called CRC-LM PDX-derived cell model, which is a CRC-LM PDC model (LIDE Biotech, Shanghai, China). Briefly, tumor specimens were digested into single cells when tumor volume of CRC-LM PDX reached about 500 mm³. Single cells from CRC-LM PDX were seeded on 96-well plates. After treatment with ITGB8-AS1-ASO with/without miRNA inhibitors for 6 days, viability of CRC-LM PDC models were measured by the ATP-TCA method with a commercial kit, CellTiter-Glo Luminescent Cell Viability Assay Kit (Promega, Madison, WI, USA, #G7573).

Statistical analysis

All data were representative of three independent experiments and analyzed by GraphPad Prism version 8.0.1 or IBM SPSS version 25 software. Data were expressed as mean ± SD. Differences between two groups were compared using two-tailed Student's t test, paired

t test, or one-way analysis of variance (ANOVA). Correlation coefficients were obtained by Pearson correlation analysis. $p < 0.05$ was considered statistically significant.

SUPPLEMENTAL INFORMATION

Supplemental information can be found online at <https://doi.org/10.1016/j.ymthe.2021.08.011>.

ACKNOWLEDGMENTS

This work was funded by the Natural Science Foundation of Fujian Province (2020J05300), the Natural Science Foundation of China (82002496, 91953114, 81761128015, 81861130370, and 31871319), and the National Major Scientific and Technological Special Project for “Significant New Drugs Development” (2020ZX09201005).

AUTHOR CONTRIBUTIONS

X.T.L. designed the experiments, performed research, analyzed data, and wrote the manuscript. S.W.Z. performed research and analyzed data. F.Y., W.L., and X.L. conceived the original ideas, supervised the study, and revised the manuscript. X.C. and J.D. helped to carry out loss- and gain-of-function assays. L.H.Z. assisted with miRNA sponge-relevant experiments and clinical sample validation. J.C.D. and G.S.H. performed the bioinformatics analyses. L.W. and J.Y. facilitated Ago2 RIP experiments and polysome profiling analysis. F.Y., X.L., and G.H.T. provided clinical samples. All authors read and approved the final manuscript.

DECLARATION OF INTERESTS

The authors declare no competing interests.

REFERENCES

- Abraham, J.M., and Meltzer, S.J. (2017). Long Noncoding RNAs in the Pathogenesis of Barrett’s Esophagus and Esophageal Carcinoma. *Gastroenterology* 153, 27–34.
- Dekker, E., Tanis, P.J., Vleugels, J.L.A., Kasi, P.M., and Wallace, M.B. (2019). Colorectal cancer. *Lancet* 394, 1467–1480.
- Slack, F.J., and Chinnaiyan, A.M. (2019). The Role of Non-coding RNAs in Oncology. *Cell* 179, 1033–1055.
- Dragomir, M.P., Kopetz, S., Ajani, J.A., and Calin, G.A. (2020). Non-coding RNAs in GI cancers: from cancer hallmarks to clinical utility. *Gut* 69, 748–763.
- Kogo, R., Shimamura, T., Mimori, K., Kawahara, K., Imoto, S., Sudo, T., Tanaka, F., Shibata, K., Suzuki, A., Komune, S., et al. (2011). Long noncoding RNA HOTAIR regulates polycomb-dependent chromatin modification and is associated with poor prognosis in colorectal cancers. *Cancer Res.* 71, 6320–6326.
- Tang, J., Yan, T., Bao, Y., Shen, C., Yu, C., Zhu, X., Tian, X., Guo, F., Liang, Q., Liu, Q., et al. (2019). LncRNA GLCC1 promotes colorectal carcinogenesis and glucose metabolism by stabilizing c-Myc. *Nat. Commun.* 10, 3499.
- Wang, Y., Lu, J.H., Wu, Q.N., Jin, Y., Wang, D.S., Chen, Y.X., Liu, J., Luo, X.J., Meng, Q., Pu, H.Y., et al. (2019). LncRNA LINRIS stabilizes IGF2BP2 and promotes the aerobic glycolysis in colorectal cancer. *Mol. Cancer* 18, 174.
- Bian, Z., Zhang, J., Li, M., Feng, Y., Wang, X., Zhang, J., Yao, S., Jin, G., Du, J., Han, W., et al. (2018). LncRNA-FEZF1-AS1 Promotes Tumor Proliferation and Metastasis in Colorectal Cancer by Regulating PKM2 Signaling. *Clin. Cancer Res.* 24, 4808–4819.
- Wang, J., Zhou, J., Jiang, C., Zheng, J., Namba, H., Chi, P., and Asakawa, T. (2019). LNRRIL6, a novel long noncoding RNA, protects colorectal cancer cells by activating the IL-6-STAT3 pathway. *Mol. Oncol.* 13, 2344–2360.
- Zhu, P., Wu, J., Wang, Y., Zhu, X., Lu, T., Liu, B., He, L., Ye, B., Wang, S., Meng, S., et al. (2018). LncGata6 maintains stemness of intestinal stem cells and promotes intestinal tumorigenesis. *Nat. Cell Biol.* 20, 1134–1144.
- Wu, Y., Yang, X., Chen, Z., Tian, L., Jiang, G., Chen, F., Li, J., An, P., Lu, L., Luo, N., et al. (2019). m⁶A-induced lncRNA RP11 triggers the dissemination of colorectal cancer cells via upregulation of Zeb1. *Mol. Cancer* 18, 87.
- Ma, Y., Yang, Y., Wang, F., Moyer, M.P., Wei, Q., Zhang, P., Yang, Z., Liu, W., Zhang, H., Chen, N., et al. (2016). Long non-coding RNA CCAL regulates colorectal cancer progression by activating Wnt/ β -catenin signalling pathway via suppression of activator protein 2 α . *Gut* 65, 1494–1504.
- Zhou, Q., Hou, Z., Zuo, S., Zhou, X., Feng, Y., Sun, Y., and Yuan, X. (2019). LUCAT1 promotes colorectal cancer tumorigenesis by targeting the ribosomal protein L40-MDM2-p53 pathway through binding with UBA52. *Cancer Sci.* 110, 1194–1207.
- Yang, M.H., Zhao, L., Wang, L., Ou-Yang, W., Hu, S.S., Li, W.L., Ai, M.L., Wang, Y.Q., Han, Y., Li, T.T., et al. (2019). Nuclear lncRNA HOXD-AS1 suppresses colorectal carcinoma growth and metastasis via inhibiting HOXD3-induced integrin β 3 transcriptional activating and MAPK/AKT signalling. *Mol. Cancer* 18, 31.
- Huang, J.Z., Chen, M., Chen, D., Gao, X.C., Zhu, S., Huang, H., Hu, M., Zhu, H., and Yan, G.R. (2017). A Peptide Encoded by a Putative lncRNA HOXB-AS3 Suppresses Colon Cancer Growth. *Mol. Cell* 68, 171–184.e6.
- Marín-Béjar, O., Marchese, F.P., Athie, A., Sánchez, Y., González, J., Segura, V., Huang, L., Moreno, I., Navarro, A., Monzó, M., et al. (2013). Pint lincRNA connects the p53 pathway with epigenetic silencing by the Polycomb repressive complex 2. *Genome Biol.* 14, R104.
- Liu, L., Wang, H.J., Meng, T., Lei, C., Yang, X.H., Wang, Q.S., Jin, B., and Zhu, J.F. (2019). lncRNA GAS5 Inhibits Cell Migration and Invasion and Promotes Autophagy by Targeting miR-222-3p via the GAS5/PTEN-Signaling Pathway in CRC. *Mol. Ther. Nucleic Acids* 17, 644–656.
- Wang, Y.Q., Jiang, D.M., Hu, S.S., Zhao, L., Wang, L., Yang, M.H., Ai, M.L., Jiang, H.J., Han, Y., Ding, Y.Q., and Wang, S. (2019). SATB2-AS1 Suppresses Colorectal Carcinoma Aggressiveness by Inhibiting SATB2-Dependent *Snail* Transcription and Epithelial-Mesenchymal Transition. *Cancer Res.* 79, 3542–3556.
- Lan, Y., Xiao, X., He, Z., Luo, Y., Wu, C., Li, L., and Song, X. (2018). Long noncoding RNA OCC-1 suppresses cell growth through destabilizing HuR protein in colorectal cancer. *Nucleic Acids Res.* 46, 5809–5821.
- Han, Q., Xu, L., Lin, W., Yao, X., Jiang, M., Zhou, R., Sun, X., and Zhao, L. (2019). Long noncoding RNA CRCMSL suppresses tumor invasive and metastasis in colorectal carcinoma through nucleocytoplasmic shuttling of HMGB2. *Oncogene* 38, 3019–3032.
- Sun, Z., Guo, S.S., and Fässler, R. (2016). Integrin-mediated mechanotransduction. *J. Cell Biol.* 215, 445–456.
- Wehrle-Haller, B. (2012). Assembly and disassembly of cell matrix adhesions. *Curr. Opin. Cell Biol.* 24, 569–581.
- Kechagia, J.Z., Ivaska, J., and Roca-Cusachs, P. (2019). Integrins as biomechanical sensors of the microenvironment. *Nat. Rev. Mol. Cell Biol.* 20, 457–473.
- Hamidi, H., and Ivaska, J. (2018). Every step of the way: integrins in cancer progression and metastasis. *Nat. Rev. Cancer* 18, 533–548.
- Deschout, H., Platzman, I., Sage, D., Feletti, L., Spatz, J.P., and Radenovic, A. (2017). Investigating Focal Adhesion Substructures by Localization Microscopy. *Biophys. J.* 113, 2508–2518.
- Desgrosellier, J.S., and Cheresch, D.A. (2010). Integrins in cancer: biological implications and therapeutic opportunities. *Nat. Rev. Cancer* 10, 9–22.
- Cooper, J., and Giancotti, F.G. (2019). Integrin Signaling in Cancer: Mechanotransduction, Stemness, Epithelial Plasticity, and Therapeutic Resistance. *Cancer Cell* 35, 347–367.
- Tang, G.H., Chen, X., Ding, J.C., Du, J., Lin, X.T., Xia, L., Lian, J.B., Ye, F., He, X.S., and Liu, W. (2020). LncRNA LUCRC Regulates Colorectal Cancer Cell Growth and Tumorigenesis by Targeting Endoplasmic Reticulum Stress Response. *Front. Genet.* 10, 1409.
- Bao, J., Chen, X., Hou, Y., Kang, G., Li, Q., and Xu, Y. (2018). LncRNA DBH-AS1 facilitates the tumorigenesis of hepatocellular carcinoma by targeting miR-138 via FAK/Src/ERK pathway. *Biomed. Pharmacother.* 107, 824–833.

30. Zhang, S., Ma, H., Zhang, D., Xie, S., Wang, W., Li, Q., Lin, Z., and Wang, Y. (2018). LncRNA KCNQ1OT1 regulates proliferation and cisplatin resistance in tongue cancer via miR-211-5p mediated Ezrin/Fak/Src signaling. *Cell Death Dis.* 9, 742.
31. He, S., Huang, Q., Hu, J., Li, L., Xiao, Y., Yu, H., Han, Z., Wang, T., Zhou, W., Wei, H., and Xiao, J. (2019). EWS-FLI1-mediated tenascin-C expression promotes tumour progression by targeting MALAT1 through integrin $\alpha 5\beta 1$ -mediated YAP activation in Ewing sarcoma. *Br. J. Cancer* 121, 922–933.
32. Piipponen, M., Heino, J., Kähäri, V.M., and Nissinen, L. (2018). Long non-coding RNA PICSAR decreases adhesion and promotes migration of squamous carcinoma cells by downregulating $\alpha 2\beta 1$ and $\alpha 5\beta 1$ integrin expression. *Biol. Open* 7, bio037044.
33. Xie, S., Yu, X., Li, Y., Ma, H., Fan, S., Chen, W., Pan, G., Wang, W., Zhang, H., Li, J., and Lin, Z. (2018). Upregulation of lncRNA ADAMTS9-AS2 Promotes Salivary Adenoid Cystic Carcinoma Metastasis via PI3K/Akt and MEK/Erk Signaling. *Mol. Ther.* 26, 2766–2778.
34. Yang, J., Jiang, B., Hai, J., Duan, S., Dong, X., and Chen, C. (2019). Long noncoding RNA opa-interacting protein 5 antisense transcript 1 promotes proliferation and invasion through elevating integrin $\alpha 6$ expression by sponging miR-143-3p in cervical cancer. *J. Cell. Biochem.* 120, 907–916.
35. Chen, S., Wu, D.D., Sang, X.B., Wang, L.L., Zong, Z.H., Sun, K.X., Liu, B.L., and Zhao, Y. (2017). The lncRNA HULC functions as an oncogene by targeting ATG7 and ITGB1 in epithelial ovarian carcinoma. *Cell Death Dis.* 8, e3118.
36. Yang, Y.X., Wei, L., Zhang, Y.J., Hayano, T., Piñeiro Pereda, M.D.P., Nakaoka, H., Li, Q., Barragán Mallofret, I., Lu, Y.Z., Tamagnone, L., et al. (2018). Long non-coding RNA p10247, high expressed in breast cancer (lncRNA-BCHE), is correlated with metastasis. *Clin. Exp. Metastasis* 35, 109–121.
37. Kang, C.L., Qi, B., Cai, Q.Q., Fu, L.S., Yang, Y., Tang, C., Zhu, P., Chen, Q.W., Pan, J., Chen, M.H., and Wu, X.Z. (2019). LncRNA AY promotes hepatocellular carcinoma metastasis by stimulating *ITGAV* transcription. *Theranostics* 9, 4421–4436.
38. Wei, C.M., Zhao, X.F., Qiu, H.B., Ming, Z., Liu, K., and Yan, J. (2020). The long non-coding RNA PVT1/miR-145-5p/ITGB8 axis regulates cell proliferation, apoptosis, migration and invasion in non-small cell lung cancer cells. *Neoplasma* 67, 802–812.
39. Zhang, X., Weissman, S.M., and Newburger, P.E. (2014). Long intergenic non-coding RNA HOTAIRM1 regulates cell cycle progression during myeloid maturation in NB4 human promyelocytic leukemia cells. *RNA Biol.* 11, 777–787.
40. Dong, L., Qian, J., Chen, F., Fan, Y., and Long, J. (2019). LINC00461 promotes cell migration and invasion in breast cancer through miR-30a-5p/integrin $\beta 3$ axis. *J. Cell. Biochem.* 120, 4851–4862.
41. Zheng, Z.Q., Li, Z.X., Zhou, G.Q., Lin, L., Zhang, L.L., Lv, J.W., Huang, X.D., Liu, R.Q., Chen, F., He, X.J., et al. (2019). Long Noncoding RNA FAM225A Promotes Nasopharyngeal Carcinoma Tumorigenesis and Metastasis by Acting as ceRNA to Sponge miR-590-3p/miR-1275 and Upregulate ITGB3. *Cancer Res.* 79, 4612–4626.
42. Li, Y., Huang, W.Q., and Chen, L.L. (2020). [LncRNA NEAT1 regulates proliferation, migration and invasion of tongue squamous cell carcinoma cells by regulating miR-339-5p/ITGA3 axis]. *Shanghai Kou Qiang Yi Xue* 29, 267–274.
43. Wang, P., Liu, G.Z., Wang, J.F., and Du, Y.Y. (2020). SNHG3 silencing suppresses the malignant development of triple-negative breast cancer cells by regulating miRNA-326/integrin $\alpha 5$ axis and inactivating Vav2/Rac1 signaling pathway. *Eur. Rev. Med. Pharmacol. Sci.* 24, 5481–5492.
44. Guo, T., Wang, H., Liu, P., Xiao, Y., Wu, P., Wang, Y., Chen, B., Zhao, Q., Liu, Z., and Liu, Q. (2018). SNHG6 Acts as a Genome-Wide Hypomethylation Trigger via Coupling of miR-1297-Mediated S-Adenosylmethionine-Dependent Positive Feedback Loops. *Cancer Res.* 78, 3849–3864.
45. Guo, H., Liu, J., Ben, Q., Qu, Y., Li, M., Wang, Y., Chen, W., and Zhang, J. (2016). The aspirin-induced long non-coding RNA OLAIP2 blocks phosphorylated STAT3 homodimer formation. *Genome Biol.* 17, 24.
46. Shi, L., Hong, X., Ba, L., He, X., Xiong, Y., Ding, Q., Yang, S., and Peng, G. (2019). Long non-coding RNA ZNFX1-AS1 promotes the tumor progression and metastasis of colorectal cancer by acting as a competing endogenous RNA of miR-144 to regulate EZH2 expression. *Cell Death Dis.* 10, 150.
47. Galamb, O., Barták, B.K., Kalmár, A., Nagy, Z.B., Szigeti, K.A., Tulassay, Z., Igaz, P., and Molnár, B. (2019). Diagnostic and prognostic potential of tissue and circulating long non-coding RNAs in colorectal tumors. *World J. Gastroenterol.* 25, 5026–5048.
48. Liang, Z.X., Liu, H.S., Wang, F.W., Xiong, L., Zhou, C., Hu, T., He, X.W., Wu, X.J., Xie, D., Wu, X.R., and Lan, P. (2019). LncRNA RPPH1 promotes colorectal cancer metastasis by interacting with TUBB3 and by promoting exosomes-mediated macrophage M2 polarization. *Cell Death Dis.* 10, 829.
49. Oehme, F., Krahl, S., Gyorffy, B., Muessle, B., Rao, V., Greif, H., Ziegler, N., Lin, K., Thepkayson, M.L., Polster, H., et al. (2019). Low level of exosomal long non-coding RNA *HOTTIP* is a prognostic biomarker in colorectal cancer. *RNA Biol.* 16, 1339–1345.
50. Xu, W., Zhou, G., Wang, H., Liu, Y., Chen, B., Chen, W., Lin, C., Wu, S., Gong, A., and Xu, M. (2020). Circulating lncRNA SNHG11 as a novel biomarker for early diagnosis and prognosis of colorectal cancer. *Int. J. Cancer* 146, 2901–2912.
51. Lin, C., and Yang, L. (2018). Long Noncoding RNA in Cancer: Wiring Signaling Circuitry. *Trends Cell Biol.* 28, 287–301.
52. Chen, J., Liu, A., Wang, Z., Wang, B., Chai, X., Lu, W., Cao, T., Li, R., Wu, M., Lu, Z., et al. (2020). LINC00173.v1 promotes angiogenesis and progression of lung squamous cell carcinoma by sponging miR-511-5p to regulate VEGFA expression. *Mol. Cancer* 19, 98.
53. Jin, X., Ge, L.P., Li, D.Q., Shao, Z.M., Di, G.H., Xu, X.E., and Jiang, Y.Z. (2020). LncRNA TROJAN promotes proliferation and resistance to CDK4/6 inhibitor via CDK2 transcriptional activation in ER+ breast cancer. *Mol. Cancer* 19, 87.
54. Pucci, P., Venalainen, E., Alborelli, I., Quagliata, L., Hawkes, C., Mather, R., Romero, I., Rigas, S.H., Wang, Y., and Crea, F. (2020). LncRNA *HORAS5* promotes taxane resistance in castration-resistant prostate cancer via a BCL2A1-dependent mechanism. *Epigenomics* 12, 1123–1138.
55. Taiana, E., Favasuli, V., Ronchetti, D., Todoerti, K., Pelizzoni, F., Manzoni, M., Barbieri, M., Fabris, S., Silvestris, I., Gallo Cantafio, M.E., et al. (2020). Long non-coding RNA NEAT1 targeting impairs the DNA repair machinery and triggers anti-tumor activity in multiple myeloma. *Leukemia* 34, 234–244.
56. Gao, W.W., Xiao, R.Q., Peng, B.L., Xu, H.T., Shen, H.F., Huang, M.F., Shi, T.T., Yi, J., Zhang, W.J., Wu, X.N., et al. (2015). Arginine methylation of HSP70 regulates retinoid acid-mediated RAR $\beta 2$ gene activation. *Proc. Natl. Acad. Sci. USA* 112, E3327–E3336.
57. Ray, P.S., Jia, J., Yao, P., Majumder, M., Hatzoglou, M., and Fox, P.L. (2009). A stress-responsive RNA switch regulates VEGFA expression. *Nature* 457, 915–919.